

CEBAF-PR-96-001
JANUARY 9, 1996

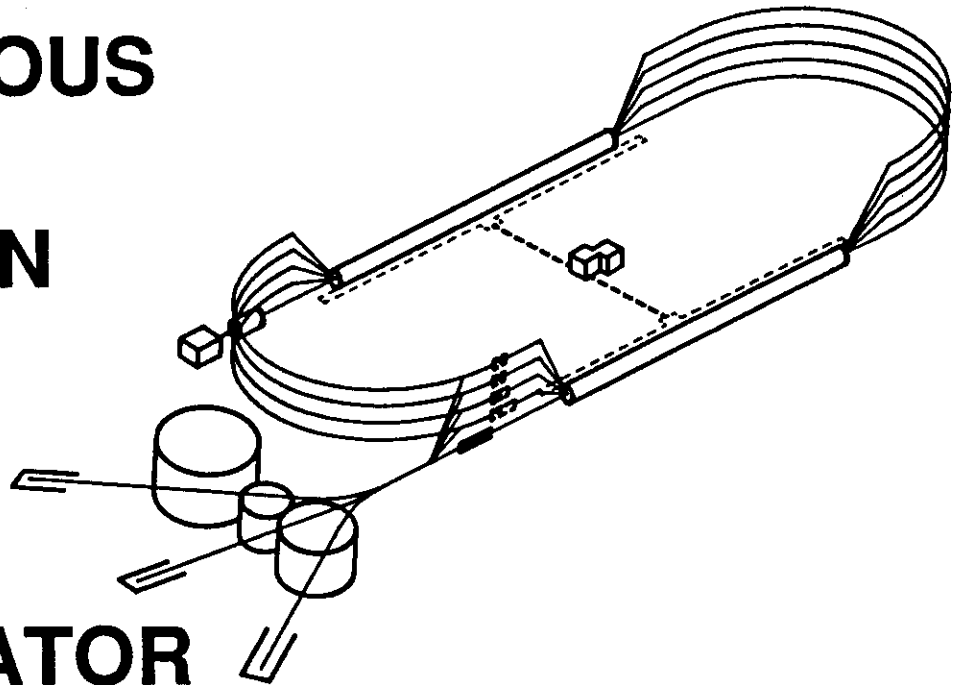
CEBAF AND THE BARYON PHYSICS PROGRAM

Volker D. Burkert
CEBAF, 12000 Jefferson Avenue, Newport News,
Virginia, 23606, USA

Invited talk at the Baryons' '95 Conference in Santa Fe,
New Mexico on October 4, 1995.

C E B A F

CONTINUOUS
ELECTRON
BEAM
ACCELERATOR
FACILITY



SURA *Southeastern Universities Research Association*

CEBAF

The Continuous Electron Beam Accelerator Facility

Newport News, Virginia

CEBAF AND THE BARYON PHYSICS PROGRAM

Volker D. Burkert

CEBAF, 12000 Jefferson Avenue, Newport News, Virginia 23606, USA

ABSTRACT

The initial complement of experimental instrumentation and the physics program at CEBAF are discussed. Using the power of the electromagnetic and neutral weak interaction, the structure of light quark baryons will be studied utilizing high duty cycle electron and photon beams with energies up to initially 4 GeV. The baryon physics program at 4 GeV is discussed, as well as future energy upgrades into the 8 - 10 GeV regime.

1. Introduction

Electron scattering as a probe of the internal structure of nucleons has been employed for several decades, mostly in inclusive reactions and using low duty cycle machines. Experiments in the deep inelastic regime revealed the quark substructure of the nucleon, and more recently showed that the spin structure of the nucleon is more complicated than originally anticipated. A more detailed understanding of the structure of nucleons the measurement of more exclusive channels. For example, the study of the excited states of the nucleon requires the identification of spin, parity, and isospin of an intermediate state, which can only be accomplished by studying the resonance decay channels. In the past, low duty cycle machines have limited exclusive experiments to a few processes, mostly single pion production, and to restricted kinematics. The construction of high current, high duty cycle electron accelerators has changed this situation in a significant way. *Electromagnetic processes may now be studied with statistical sensitivities comparable to hadronic reactions.* This brings to bear the full capability of the electromagnetic interaction as a probe of the internal structure of hadrons.

2. The Accelerator and the Initial Experimental Equipment

The CEBAF electron accelerator is based on superconducting rf cavities operated in a continuous wave (cw) mode. A schematic of the machine is shown in Fig. 1. Two parallel linacs in a "race track" configuration boost the beam energy by 800 MeV for each turn. The beam is recirculated five times to reach an initial maximum energy of 4 GeV. The heart of the machine are the five-cell niobium cavities, which have a minimum gradient of 5 MeV per meter. The cavities perform significantly better than the specifications, therefore providing the technical basis for a future energy upgrade. The machine can deliver electrons to 3 experimental areas (Hall A, B, C) at either the same energy, or at multiples of 1/5 of the end energy. Due to the virtual lack of synchrotron radiation, the energy spread in the beam is $\Delta E/E \leq 10^{-4}$.

Beams can be extracted at each recirculation, thus allowing the operation of the experimental halls with simultaneous beams of different, though correlated, energies. The 1.5 GHz rf structure allows simultaneous beams to be delivered to the halls at a frequency of 500 MHz. The micro bunches can also be loaded with different electron densities, which provides the basis for operating the experimental areas with currents spanning a large dynamic range.

In addition, a polarized electron gun can be operated in parallel with the standard thermionic unpolarized gun.

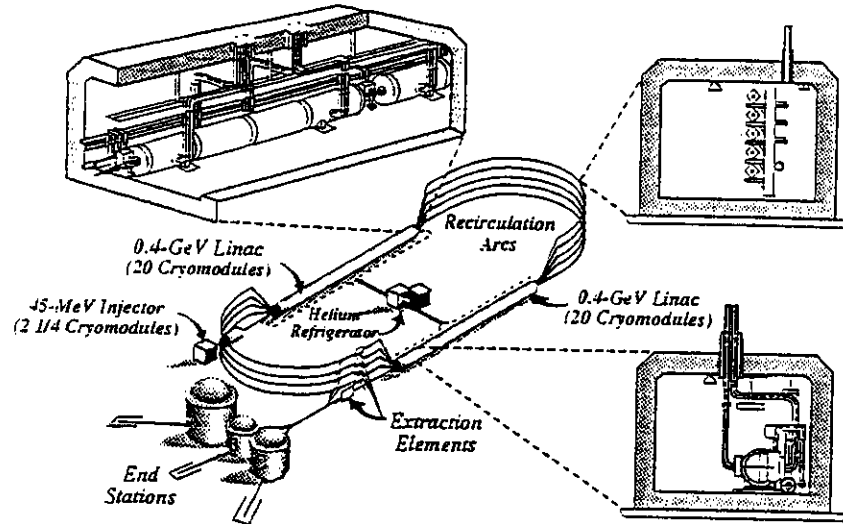


Figure 1: Schematics of the CEBAF accelerator.

The halls are equipped with spectrometers for complementary experimental programs (Fig. 2). Hall C, which is already fully instrumented, contains two magnetic spectrometers of medium resolution with $\delta p/p \leq 10^{-3}$ but different maximum momenta: the High Momentum Spectrometer (HMS) has a maximum momentum of 7 GeV/c, and the Short Orbit Spectrometer (SOS) of 1.8 GeV/c, respectively.

Hall A will house two high resolution spectrometers (HRS) with $\delta p/p \leq 10^{-4}$ and a maximum momentum of 4 GeV/c, instrumented for electron and hadron detection, respectively. The spectrometers are expected to be operational in spring 1996.

Hall B will house the CEBAF Large Acceptance Spectrometer (CLAS) and a tagged photon facility. CLAS is based on a multi-gap magnet with six superconducting coils, symmetrically arranged to generate an approximately toroidal magnetic field distribution. Each of the six sectors is instrumented with drift chambers, time-of-flight counters, Cerenkov counters for electron identification, and electromagnetic calorimetry for photon and neutron detection. Completion of hall B is expected in the fall of 1996.

3. Structure of the Nucleon.

The structure of the nucleon may be probed in elastic electron nucleon scattering and in inelastic reactions induced by electrons or photons. These experiments measure the charge and current distribution of the nucleons and the transition currents to their excited states. Knowledge of these quantities allows testing of models describing the nucleon structure at low and intermediate energy and momentum transfer. With increasing momentum transfer Q^2 , the transition from the non-perturbative regime to the perturbative regime can be studied, where simple quark counting rules and power law behavior may apply.¹

More than half of all approved experiments at CEBAF address questions related to

the structure of light baryons and mesons some of which either require measurement of spin observables, or the sensitivity to fundamental quantities is increased significantly in spin observables. Polarized electron beams, polarized targets, and proton and neutron recoil polarimeters will be important tools in these studies.

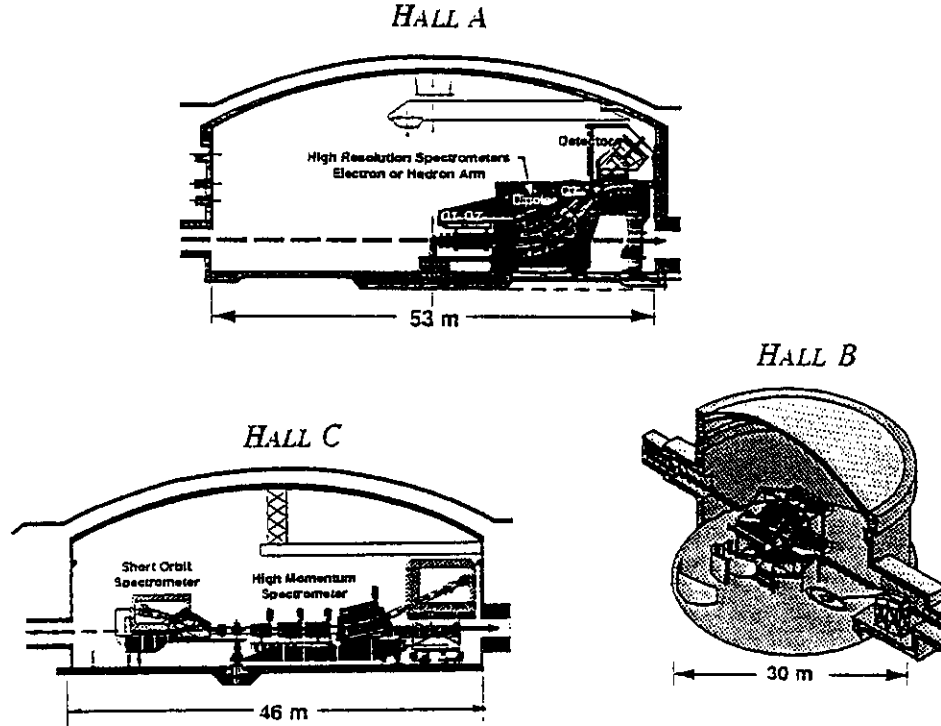


Figure 2: The initial equipment in the experimental halls

3.1. Electromagnetic Form Factors.

In elastic electron nucleon scattering the hadronic current may be specified by the electric and magnetic form factors $G_E(Q^2)$ and $G_M(Q^2)$. The usual technique for measuring the elastic form factors is the Rosenbluth separation, where one makes use of the different angular dependence of the electric and the magnetic term in the unpolarized elastic cross section to separate $|G_E|$ and $|G_M|$.

$$\frac{d\sigma}{d\Omega} = \left(\frac{d\sigma}{d\Omega}\right)_M \frac{E'}{E} [(G_E^2 + \tau G_M^2) + 2\tau(1 + \tau)G_M^2 \tan^2 \frac{\theta}{2}] \quad (1)$$

where $\tau = \frac{Q^2}{4M^2}$. This technique ceases to be useful, when either $G_E^2 \ll G_M^2$, or at high values of Q^2 , where the magnetic contribution dominates both the angular dependent and the angular independent term. Unlike for the proton, the Rosenbluth separation of G_E^n from G_M^n for a neutron target is difficult even at low Q^2 , because of the small size of G_E^n compared

to G_M^n . At $Q^2 < 1 \text{ GeV}^2$, G_E^n has been extracted from elastic electron-deuteron scattering data assuming a model for the deuteron structure.²

A model-independent determination of G_E^n can be obtained by measuring the polarization asymmetry

$$A_{en} = \frac{2\tau \cos\theta v_T' + 2\sqrt{2\tau(1+\tau)} \cdot (G_E^n/G_M^n) \sin\theta \cos\phi v_{TL}'}{v_L(1+\tau)(G_E^n/G_M^n)^2 + 2\tau v_T} \quad (2)$$

where v_L, v_T, v_T', v_{TL}' are known kinematic quantities and ϕ and θ define the orientation of the nucleon spin relative to the scattering plane. From the asymmetry, the ratio G_E^n/G_M^n can be extracted. Knowing G_M^n , the electric form factor can be determined. One method uses a polarized deuterium or ^3He target, either as an ultra thin gas target in an electron storage ring, or a solid state target ND_3 , or a dense ^3He gas target, in an external electron beam. If the polarization asymmetry is measured using vector polarized deuterium, it will be necessary to measure the recoil neutron in coincidence with the scattered electron to eliminate the much larger contributions from the polarized proton in the deuteron. The binding of the neutron in the deuteron has negligible effect on the polarization asymmetry and on G_E^n/G_M^n , as long as the recoil neutron is emitted at small angles with respect to the direction of the virtual photon.³

A second method uses an unpolarized deuterium target, and the polarization of the recoiling neutron is measured in a second scattering experiment.

Both methods will be employed at CEBAF⁴ to measure G_E^n/G_M^n for Q^2 up to 2-3 GeV^2 (Fig. 3). In both cases, the scattered electron will be detected in the hall C HMS spectrometer, and the neutron will be detected in a narrow cone around the direction of the virtual photon. One experiment uses a polarized ND_3 solid state target, while the other one uses a plastic scintillator based polarimeter to measure the polarization of the recoil neutron.

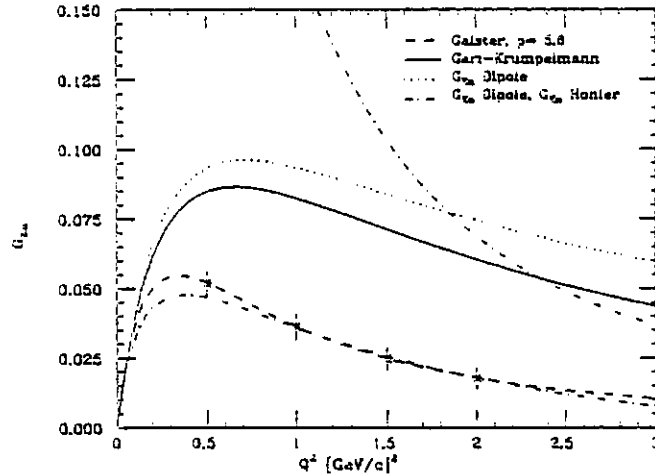


Figure 3: Projected data for a measurement of G_E^n using a polarized ND_3 solid state target

The polarization techniques can also be employed to measure the electric form factor G_E^p of the proton. Most promising in this respect is the recoil polarization techniques using an unpolarized hydrogen target.⁵ With a 4 GeV beam G_E^p can be measured for Q^2 up to 5 GeV^2 , with statistical errors of less than 5%.

Our knowledge of the magnetic form factor of the neutron is also unsatisfactory. Quasi-elastic electron scattering off deuterons appears to be the most promising way to determine G_M^n at high momentum transfers. Two experiment will measure G_M^n over a large Q^2 range.⁶ A common problem is how to determine the neutron detection efficiency accurately. A large acceptance detector such as CLAS offers the possibility to determine the efficiency by measuring the reaction $p(e, e'\pi^+)n$ using a hydrogen target, simultaneously. The neutron kinematics is completely constrained in this reaction, and can be used to determine the neutron detection efficiency. The ratio of quasi-free e-n and e-p coincidences allows to determine G_M^n using the known proton form factors as normalization.

3.2. Baryon Resonance Transitions.

A large number of resonances, attributed to the excitation of the nucleon have been observed in hadron scattering, the $\Delta(1232)$ being the most prominent one. Electromagnetic excitation of the resonances addresses fundamental questions about the interaction of quarks and gluons in confined systems. Specifically, one would like to study how the transition between the 3-quark ground state and excited states is mediated. Measurement of the Q^2 evolution of the transition form factors provides information about the wave function of the excited state. At high momentum transfer, one may observe the transition from the non-perturbative regime of QCD to the perturbative regime. A complete program to study nucleon resonance transitions involves measurement of polarization observables.

The lowest mass resonant state, the $\Delta(1232)$ is of special interest. In $SU(6)$ symmetric quark models, this transition is explained by a simple quark spin-flip in the $L_{3Q} = 0$ ground state, corresponding to a magnetic dipole transition M_{1+} . In QCD based models, which include color magnetic interactions arising from the one-gluon exchange, the $\Delta(1232)$ acquires an $L_{3Q} = 2$ component, leading to small electric and scalar contributions (e.g. $|E_{1+}/M_{1+}| \simeq 0.01$ at $Q^2 = 0$). The ratio $|E_{1+}/M_{1+}|$ is predicted to be weakly dependent on Q^2 .

Experiments at CEBAF are in preparation to measure the electromagnetic transition amplitudes for the nucleon to the Δ ,⁷ as well as to many higher mass resonances,⁸ over a large Q^2 range, using both unpolarized pion and eta electroproduction, as well as polarized electron beams and polarized targets or recoil polarimeters.⁹ For the $N\Delta$ transition one obtains information about the terms

$$M_{1+}, \text{Re}(E_{1+}M_{1+}^*), \text{Re}(S_{1+}M_{1+}^*), \text{Im}(E_{1+}M_{1+}^*), \text{Im}(S_{1+}M_{1+}^*).$$

Projected data for the $\Delta(1232)$ are shown in Fig. 4. The imaginary parts of the bilinear terms can be measured using polarization degrees of freedom.

Of topical interest are the transition form factors to the $N(1440)$, a candidate for a state with a large gluonic content.¹⁰ Gluonic excitations of baryons are not distinguished by exotic quantum numbers from ordinary baryons. Electroproduction of these states may be the only available tool in the search for signatures of these states, as their transition form factors are expected to have very different Q^2 dependence.¹⁰

The QCD motivated extension of the non-relativistic quark model¹¹ predicts many states which have not been observed in πN reactions. Several of these states are predicted to couple strongly to photons (real or virtual) and may thus be searched for in photoproduction or electroproduction experiments. Search for some of these states in multi-pion and vector meson production are in preparation at CEBAF.¹² Virtual Compton scattering off nucleons

$p(e, e'p)\gamma$ is also sensitive to the excitation of nucleon resonances and will be measured in an experiment using the HRS spectrometers.¹³ One advantage is the absence of final state interaction, while the low rate makes it difficult to achieve sufficient kinematical coverage for a complete partial wave analysis.

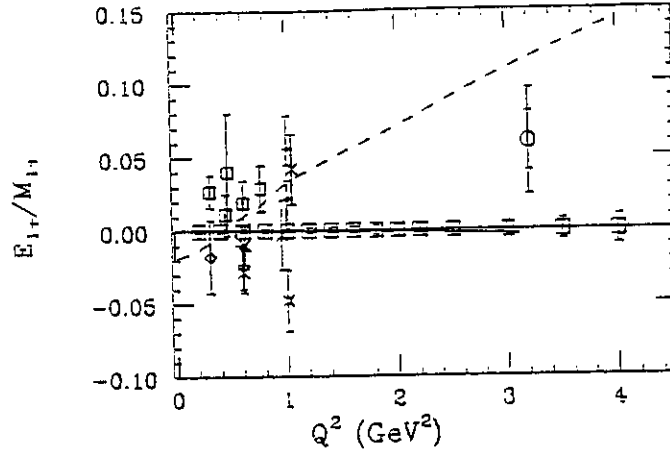


Figure 4: Data for E_{1+}/M_{1+} compared to quark model calculations. The error bars on the horizontal axis are projections of experiment E-89-037.

3.3. Parity Violation Experiments.

At low and medium energy ($Q^2 \ll M_{Z^0}^2$) neutral current interactions, the parity violating contributions arise from the interference between the one-photon exchange and the neutral weak boson Z^0 exchange graphs.

Parity violation in $\bar{e}p - ep$ probes the strange vector current $\bar{s}\gamma_\mu s$. Sizeable $s\bar{s}$ contributions in the proton are suggested by the results of the polarized structure function experiments. The parity violating asymmetry in elastic ep scattering is given by:

$$A_{\bar{e}p} \simeq \frac{G_F Q^2}{\pi \alpha \sqrt{2}} \frac{\epsilon G_E^p G_E^Z + \tau G_M^p G_M^Z}{\epsilon (G_E^p)^2 + \tau (G_M^p)^2} \quad (4)$$

In the Standard Model of particle physics:

$$G_{E,M}^Z = \left(\frac{1}{2} - \sin^2 \theta_W\right) G_{E,M}^p - \frac{1}{4} (G_{E,M}^n + G_{E,M}^s) \quad (5)$$

where $G_{E,M}^{p,n}$ are the usual electromagnetic form factors, and $G_{E,M}^Z$ are the neutral weak form factors. At large electron scattering angles the first term dominates. G_E^Z , G_M^Z can be separated by varying the electron kinematics and G_E^s , G_M^s can be determined using the known electromagnetic form factors.

Three experiments are in preparation at CEBAF to study parity violation in elastic electron scattering experiments.¹⁷ Some of the projected data are shown in Fig. 5.

3.4. Q^2 Evolution of the Nucleon Spin Structure

The study of the spin structure of the nucleon has focussed on the short distance behavior where the measurements may be interpreted in terms of the parton structure of the nucleon. Studies of the Q^2 evolution of the spin structure functions g_1 and g_2 down to small

Q^2 will give important constraints on the models aimed at describing the nucleon structure at larger distances. At $Q^2 = 0$, the Gerasimov-Drell-Hearn (GDH) sum rule constrains the slope of Γ_1 to the anomalous magnetic moment of the target:

$$\frac{2M}{Q^2}\Gamma_1 - -\frac{1}{4}\kappa^2 \quad (6)$$

The negative value is in conflict with a simple extrapolation from the deep inelastic regime.

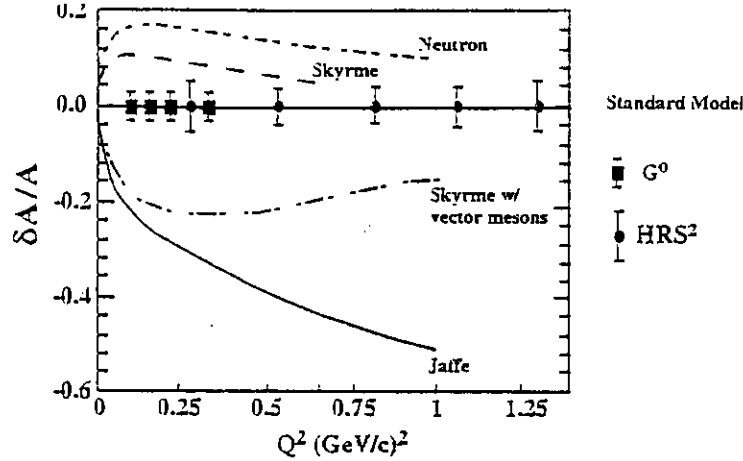


Figure 5: Projected data for the polarized electron asymmetry $p(\bar{e}, e')p$.

The GDH sum rule and its Q^2 evolution have never been studied experimentally. The only empirical information comes from the analysis of pion photo- and electroproduction experiments.^{15,16} There are plans to measure the sum rule at $Q^2 = 0$ for the protons and neutrons¹⁸ using a circularly polarized photon beam and a polarized solid state target. The Q^2 evolution will be studied in three experiments¹⁹ using polarized NH_3 , ND_3 , and 3He targets, respectively. With information on the proton and neutron, the evolution of the Bjorken integral $\Gamma_1^p - \Gamma_1^n$ can be studied down to $Q^2 = 0$, where it should be constraint by the respective difference of the GDH sum rules. Fig. 6 shows projected data on the double polarization asymmetry using a NH_3 target.

3.5. Strangeness Production

Electromagnetic production of strange particles $\gamma p \rightarrow K^+ Y$ ($Y = \Lambda, \Lambda^*, \Sigma, \Sigma^*$) have been poorly studied in the past. Consequently, the production mechanism is not well understood. In a diagrammatic approach the process is sensitive to the $K\Lambda N$ and $K\Lambda N^*$ coupling constants. Coupling constants extracted from photoproduction data and from hadronic data disagree. Calculations indicate that the Λ polarization is very sensitive to specific ingredients of the model, in particular on assumptions about the coupling constants. Measurement of the Λ recoil polarization in photoproduction reactions will thus yield independent information about the hadronic coupling constants.

An efficient experimental program to study polarization degrees of freedom in the $K\Lambda$ channel benefit greatly from the use of large acceptance detectors with nearly 4π solid angle coverage. For example, the Λ polarization can be inferred from an analysis of $\Lambda \rightarrow \pi^- p$ decay.

Using a longitudinally polarized electron beam, circularly polarized bremsstrahlung photons can be generated, and the polarization transfer reaction $\bar{\gamma}p \rightarrow K\bar{\Lambda}$ can be studied as well.

CLAS experiments will cover hyperon photoproduction on the proton²¹ and deuteron,²² and hyperon electroproduction.²³ Fig. 7 shows the expected missing mass distribution in $\gamma p \rightarrow K^+ X$ for a proton target. The Λ , Σ^0 , $\Lambda(1520)$, and a combination of $\Lambda(1405)$ and $\Sigma^0(1385)$ can be isolated.

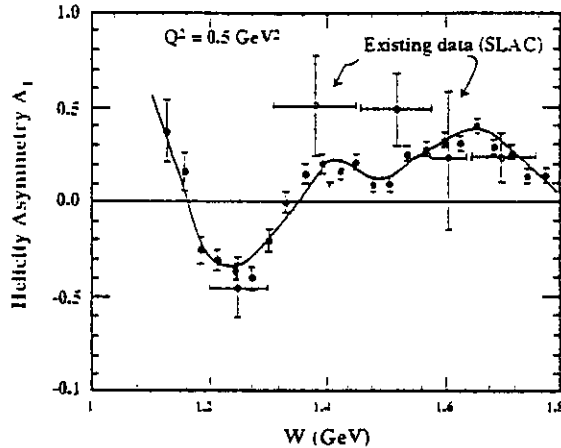


Figure 6: Projected data (full circle) on the double polarization asymmetry $\bar{p}(\bar{e}, e')X$ at fixed Q^2 .

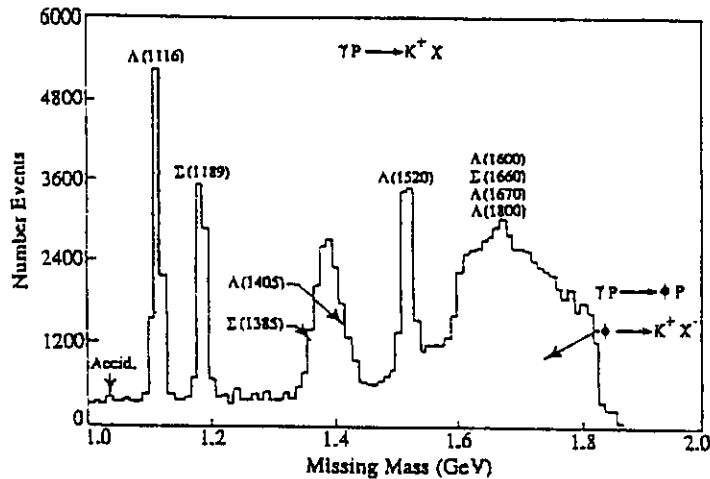


Figure 7: Missing mass distribution for $\gamma p \rightarrow K^+ X$.

4. CEBAF Energy Upgrade

Based on the better than expected performance of the superconducting cavities, there is an excellent possibility that the maximum energy of the accelerator can be upgraded to about 6 GeV in 1997. This will be accomplished largely by increasing the rf power to the cavities, and by upgrading the power supplies of the dipole magnets in the recirculation arcs.

This will allow to increase the available Q^2 range to about 6 - 7 GeV^2 for the study of form factors, and probe part of the deep inelastic regime.

A further energy upgrade into the 8 to 10 GeV energy regime has been proposed,²⁴ and appears feasible with relatively modest financial investment. This would be accomplished by installing additional accelerating cavities in the accelerator tunnel, and by replacing cavities with low field gradients with better performing ones. Additional upgrades of magnets and power supplies in the arcs will be necessary as well. The total cost of this upgrade is estimated to be about \$30M. Such an energy upgrade would allow measurements of form factors for Q^2 well beyond 10 GeV^2 . It would also open up new possibilities to study production and decays of heavy mesons, such as the predicted gluonic excitations, and strangeonium (ϕ^*). Measurement of higher moments of the spin structure functions of the nucleon such as $\int x^2 g_1(x, Q^2)$ would be feasible, yielding new information about the nucleon spin structure functions. It would also provide full access to the deep inelastic regime.

5. Summary and Outlook.

The CEBAF electron accelerator is a powerful tool in probing the internal structure of baryons with unprecedented precision. The initial experimental equipment has been designed for complementary experimental programs. Already from the initial experimental program we expect significant insight into the manifestation of QCD in the confinement regime.

As of November 1995, the accelerator has reached 5 recirculations and a 4 GeV cw beam was delivered to hall C. The first nuclear physics experiments has started in mid-November. Completion of the hall A equipment is expected for spring 1996, and the instrumentation in hall B should be operational by the end of 1996.

References

1. S. J. Brodsky and G. P. Lepage, *Phys. Rev. D* **24**, 2848 (1981)
2. S. Platchkov et al., *Nucl. Phys. A* **510**, 740 (1990)
3. H. Arenhövel, W. Leidemann, and E.L. Tomusiak, *Z. Phys. A* **331**, 123 (1988)
4. CEBAF experiments E-93-026, E-93-038
5. CEBAF experiment E-93-027.
6. CEBAF experiments E-93-024, E-94-017
7. CEBAF experiments E-89-037, E-89-042, E-94-014
8. CEBAF experiments E-89-038, E-89-039, E-91-002
9. CEBAF experiments E-91-011, E-93-036
10. Z.P. Li, V. Burkert, Zh. Li, *Phys. Rev. D* **46**, 70(1992).
11. N. Isgur and G. Karl, *Phys. Lett.* **72B**, 109 (1977); *Phys. Rev. D* **23**, 817 (1981)
12. CEBAF experiments E-91-024, E-93-006, E-93-033, E-94-109
13. CEBAF experiment E-93-050
14. CEBAF experiment E-93-021
15. I. Karliner, *Phys. Rev. D* **7**, 2717 (1973)
16. V. Burkert and Zh. Li, *Phys. Rev. D* **47**, 46(1993)
17. CEBAF experiments E-91-004, E-91-010, E-91-017
18. CEBAF experiment E-91-015, PR-94-117
19. CEBAF experiment E-91-023, E-93-009, E-94-010
20. CEBAF experiment E-89-043
21. CEBAF experiments E-89-004, E-89-024
22. CEBAF experiment E-89-045
23. CEBAF experiment E-93-030
24. CEBAF at Higher Energies A White Paper, February 1995